

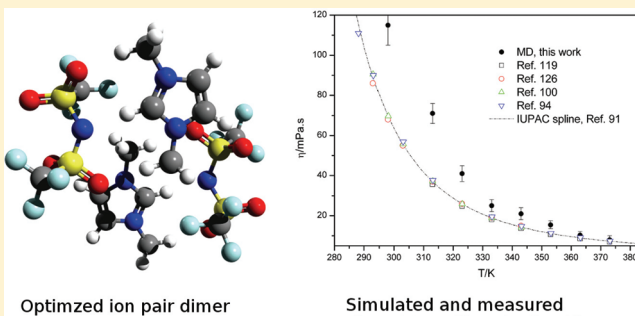
Improved Classical United-Atom Force Field for Imidazolium-Based Ionic Liquids: Tetrafluoroborate, Hexafluorophosphate, Methylsulfate, Trifluoromethylsulfonate, Acetate, Trifluoroacetate, and Bis(trifluoromethylsulfonyl)amide

Xiujuan Zhong, Zhiping Liu,* and Dapeng Cao*

Division of Molecular and Materials Simulation, State Key Laboratory of Organic–Inorganic Composites, Beijing University of Chemical Technology, Beijing 100029, China

 Supporting Information

ABSTRACT: A cost-effective, classical united-atom (UA) force field for ionic liquids (ILs) was proposed, which can be used in simulations of ILs composed by 1-alkyl-3-methyl-imidazolium cations ($[C_n\text{mim}]^+$) and seven kinds of anions, including tetrafluoroborate ($[\text{BF}_4]^-$), hexafluorophosphate ($[\text{PF}_6]^-$), methylsulfate ($[\text{CH}_3\text{SO}_4]^-$), trifluoromethylsulfonate ($[\text{CF}_3\text{SO}_3]^-$), acetate ($[\text{CH}_3\text{CO}_2]^-$), trifluoroacetate ($[\text{CF}_3\text{CO}_2]^-$), and bis(trifluoromethylsulfonyl)amide ($[\text{NTf}_2]^-$). The same strategy in our previous work (*J. Phys. Chem. B* 2010, 114, 4572) was used to parametrize the force field, in which the effective atom partial charges are fitted by the electrostatic potential surface (ESP) of ion pair dimers to account for the overall effects of polarization in ILs. The total charges (absolute values) on the cation/anion are in the range of 0.64–0.75, which are rescaled to 0.8 for all kinds of ions by a compromise between transferability and accuracy. Extensive molecular dynamics (MD) simulations were performed over a wide range of temperatures to validate the force field, especially on the enthalpies of vaporization (ΔH^vap) and transport properties, including the self-diffusion coefficient and shear viscosity. The liquid densities were predicted very well for all of the ILs studied in this work with typical deviations of less than 1%. The simulated ΔH^vap at 298 and 500 K are also in good agreement with the measured values by different experimental methods, with a slight overestimation of about 5 kJ/mol. The influence of ΔC_p (the difference between the molar heat capacity at constant pressure of the gas and that of liquid) on the calculation of ΔH^vap is also discussed. The transport coefficients were estimated by the equilibrium MD method using 20–60 ns trajectories to improve the sampling. The proposed force field gives a good description of the self-diffusion coefficients and shear viscosities, which is comparable to the recently developed polarizable force field. Although slightly lower dynamics is found in simulations by our force field, the order of magnitude of the self-diffusion coefficient and viscosity are reproduced for all the ILs very well over a wide temperature range. The largest underestimation of the self-diffusion coefficient is about one-third of the experimental values, while the largest overestimation of the viscosity is about two times the experimental values.



1. INTRODUCTION

Ionic liquids (ILs) are molten salts at room temperature, composed of only cations and anions. In recent years, they have received tremendous attention by both the academic and the industrial community because of their remarkable properties, such as extremely low vapor pressure, wide electrochemical window, high ionic conductivity, and good thermal and chemical stability.^{1–3} More importantly, their properties can be tailored for specific applications^{4–9} by different combinations of cations and anions or introducing functional groups to the ion. Due to their wide range of properties, the potential applications on many important fields³ were reported, including synthesis and catalysis,^{1,10} solar cells,^{11,12} carbon dioxide capture,^{4,8,13–15} biomass processing,^{16–19} and nanomaterials preparation and separation.^{20,21}

The traditional trial-and-error way to find new ILs or optimize their combinations leads to the large cost on the syntheses and experiments. Computer simulations provided an alternative and effective way in screening a large number of candidate materials.^{22–24} Among them, molecular dynamics (MD) simulations on the atomistic level were widely used in predicting both the static and the dynamic properties of various systems from simple liquids to complicated biomolecules.^{25–28} However, the quality of such simulation depends on the force field by which the interactions between atoms or molecules are defined.

Received: May 4, 2011

Revised: July 12, 2011

Published: July 14, 2011

At present, the force fields are already available for ILs,^{29–44} covering a broad set of cations and anions. Most of them were established by extending and refining the well-developed force fields, such as AMBER, CHARMM, OPLS, and GROMOS. Although many valuable results have been obtained by molecular simulations using these force fields,^{27,45–47} it is still a challenging task to predict both thermodynamic properties and the transport coefficients comparable to the experimental data.^{26,48} For example, a much slower dynamics behavior (low self-diffusion coefficient and high viscosity) was usually found when the nonpolarizable force fields were used in the simulations.^{49,50}

Significant improvement can be made by introducing polarizability to the force field. Typically, a factor of 2–4 was reported for the self-diffusion coefficient because the long-range electrostatic interactions are reduced by the polarization. The first polarizable force field of ILs was proposed by Yan et al. for 1-ethyl-3-methyl-imidazolium nitrate ($[C_2mim][NO_3]$) based on the atomic induced dipole model.⁵¹ Recently, they compared the simulation results in detail with both the polarizable and the nonpolarizable force fields.^{52,53} The self-diffusion coefficients were about 3 times larger and the viscosity 60% lower after introducing polarizability.⁵³ They also found that polarization had a different effect on short-range and long-range electrostatic interactions.⁵² The polarizable model exhibited enhanced hydrogen bonding in short-range while less ordered in long-range spatial correlations. Borodin et al. developed systematically the polarizable force field of ILs by a similar method.^{54–56} The simulation results showed very good agreement with experimental data. Comparisons of five different ILs by switching on/off the polarization in the force field showed that the dynamics was enhanced 2–4 times by polarization.⁵⁵ They also reported a factor of 4 on computational cost using a polarizable force field compared with the corresponding nonpolarizable one.⁵⁶ Other implements of polarization in the force field were also reported for ILs, such as Drude oscillator,⁵⁷ point dipole,⁵⁸ charge equilibration (Q_{eq}),⁵⁹ and the quantum mechanical wave function-based model.⁶⁰

An alternative remedy is reducing the total ion charges. Youngs and Hardacre⁶¹ showed that the dynamics of ILs was dramatically accelerated by linearly scaling down the partial charges on each atom in the nonpolarizable force field. In the simulations of $[C_1mim][Cl]$ at 450 K, more than a 30 times larger value of the self-diffusion coefficient was found after a scaling factor of 0.8 was used. It is not strange because the reduced partial charges can mimick the average charge screening caused by the polarization as well as the charge transfer effects, resulting in an effective force field implicitly including polarization. Morrow and Maginn³⁵ assigned the charges via the electrostatic potentials using a grid-based (CHELPG) fitting to the ab initio calculation of isolated ion pairs, in which the total ion charges are $\pm 0.904e$. A similar strategy was used by Lee et al.⁶² and Logothetis et al.,⁶³ and the simulation results were in good agreement with experimental measurements. For example, Logothetis et al. reported an average deviation of the self-diffusion coefficients of only about 13% in the simulations of ILs 1-alkyl-3-methyl-imidazolium bis(trifluoromethylsulfonyl)imide ($[C_nmim][NTf_2]$).⁶³ Bhargava and Balasubramanian proposed an optimized force field of $[C_4mim][PF_6]$,⁶⁴ in which $\pm 0.8e$ was chosen as the total ion charges and the partial charges were adjusted by hand. Their simulated densities of the liquids, self-diffusion coefficients, and surface

tension coincided with the experimental value very well,⁶⁴ while the viscosity was underestimated about 25–40%.⁶⁵ Klahn proposed a force field^{66,67} for the guanidinium ILs based on the charge distribution of actual liquid. They used a combined quantum mechanical/molecular mechanical (QM/MM) approach and found an average charge transfer of 0.12–0.06e from the anions to the cations. The self-diffusion coefficients at 450 K were 2–3 times those predicted by the charge distribution based on isolated ions. Recently, Roy and Maroncelli⁶⁸ also showed that the method of reducing total ion charges can improve significantly the dynamics properties of IL in their coarse-grained model.

It should be noted here that it is also possible to optimize a nonpolarizable force field without reducing the total ion charges, because the short-range interactions also have a noticeable effect on transport coefficients. For example, Köddermann et al. proposed a new force field of ILs $[C_nmim][NTf_2]$ ⁶⁹ based on those developed by Lopes et al.³¹ The partial charges remained the same, and only the Lennard–Jones (LJ) parameters were adjusted significantly. The agreement with experimental measurements was very good, including the liquid densities, heats of vaporization, self-diffusion coefficients, and viscosities. Micaelo et al. developed a united-atom (UA) force field of $[C_4mim][PF_6]$ and $[C_4mim][NO_3]$ ⁴⁴ in the framework of GROMOS96 with a good description of the liquid densities, self-diffusion coefficients, and viscosities, while the predicted heat of vaporization of $[C_4mim][NO_3]$ was substantially lower than recently reported experimental data.⁷⁰

Recently, we proposed an improved UA force field for $[C_nmim][Cl]$,⁷¹ in which the charge distribution was derived from the restraint electrostatic potential (RESP) fitting⁷² to the ab initio calculations of ion pair dimers. As a compromise between transferability and accuracy, the force field was simplified by scaling the total ion charges to $\pm 0.8e$, which is independent of the length of alkyl in the cation. The force field gave a much better description of the self-diffusion coefficients and viscosities than our previously developed UA force field.³⁹

As mentioned above, the transport and thermodynamic properties of ILs can be reproduced with fairly good accuracy by a nonpolarizable force field with reduced total ion charges. However, the transferability would be a problem in extending such kind of force field due to the many body nature of the polarization. For example, the value of total ion charges depended on the type of ILs in some of the recently published force field.^{53,66} It is also the reason why we used further scaling to achieve transferability in the force field of $[C_nmim][Cl]$.⁷¹ Very recently, Holm and co-workers analyzed the Car–Parrinello MD⁷³ results of 30 ion pairs of $[C_1mim][Cl]$ using a charge-fitting procedure due to Blöchl, which is suitable for calculation under periodic boundary conditions and also consistent with the commonly used ESP fitting method. A rather broad charge distribution centered around $0.63e$ with a root-mean-square deviation of $0.08e$ was reported for the chloride, which reflects the anisotropic local environment around the ions. Therefore, they suggested⁷⁴ that reparametrization of the short-range interactions would be usable in developing nonpolarizable force field with reduced charges.

The purpose of this work is to extend our previously proposed nonpolarizable UA force field $[C_nmim][Cl]$ ⁷¹ to other anions, including tetrafluoroborate ($[BF_4]^-$), hexafluorophosphate ($[PF_6]^-$), methylsulfate ($[CH_3SO_4]^-$), trifluoromethylsulfonate ($[CF_3SO_3]^-$), acetate ($[CH_3CO_2]^-$),

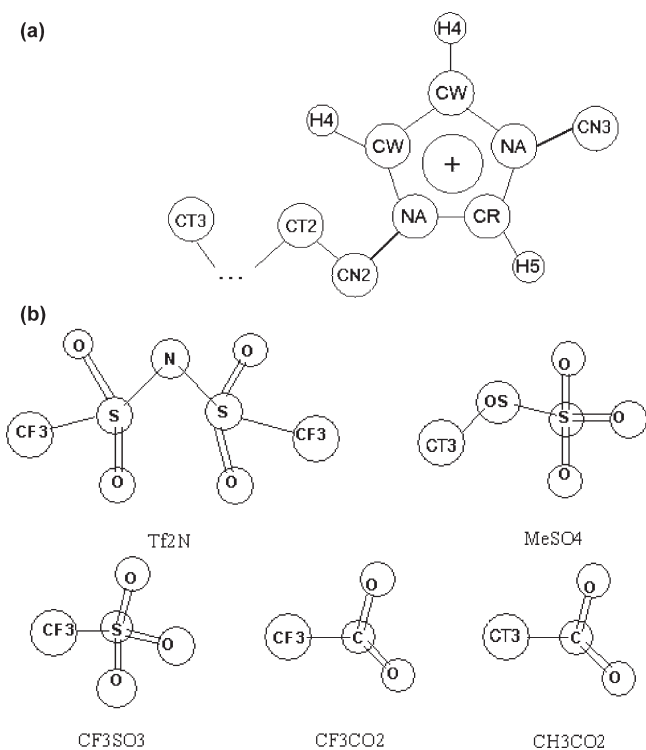


Figure 1. Schematic structure and atom-type notations of 1-alkyl-3-methyl-imidazolium cation (a) and anions (b) in this work.

trifluoroacetate ($[CF_3CO_2]^-$), and bis(trifluoromethylsulfonyl)amide ($[NTf_2]^-$). The schematic structures of these ions are shown in Figure 1. The groups of CH_2 , CH_3 , and CF_3 are treated as united atoms while all hydrogens in the imidazolium ring are not, due to the presence of hydrogen bonding in the liquid state, as indicated by both experimental⁷⁵ and theoretical⁷⁶ studies. Typically, the UA model for ILs decreases the computational cost by a factor of 1/4 or less³⁹ as compared with the corresponding all-atom (AA) force field. The partial charges derived from RESP fitting to ion pair dimers were rescaled to $\pm 0.8e$ for all kinds of ions by a compromise between transferability and accuracy. To validate the force field, the liquid densities, heats of vaporization, self-diffusion coefficients, and viscosities of a variety of ILs were calculated by extensive MD simulations. Very good agreement between simulated and experimental values was achieved. The force field also showed good performance on the temperature dependence and alkyl chain (on the cation) length dependence of these properties.

2. FORCE FIELD DEVELOPMENT

2.1. Strategy of Parametrization. The motivation of this work is to propose a transferable, computationally efficient nonpolarizable force field of imidazolium-based ILs by which both the static and the dynamic properties can be reliably predicted. The reduced ion charges were used in the force field to account for the average polarization effect in the liquid state. As a result, the dynamic properties of ILs were in much better agreement with experimental values. However, the values of the reduced ion charges would be different for the same cation/anion when they were in combination with

different counterion to form ILs because the average polarization effect depends on the type of ILs. A simple scaling method was successfully applied for $[C_n\text{mim}][\text{Cl}]$ in our previous work⁷¹ and extended to ILs with seven other anions in this work. The value of $\pm 0.8e$ was found to give good performance for all these ILs. Therefore, the transferability of the atom partial charges was achieved.

It was found that the simulated properties of ILs were sensitive to the van der Waals (vdW) parameters. However, the present force field of ILs was developed in the framework of AMBER/OPLS. Thus, it is necessary to be consistent with other parameters in these force fields. In this work, we extracted the parameters from the general AMBER force field (GAFF)⁷⁷ as much as possible. As a result, the vdW parameters in the present force field were the same as in AMBER, except the pseudo-united-atoms and the ring hydrogen atoms (see explanations in section 2.5). It is especially useful to keep consistency with the well-developed GAFF when studying the mixtures of ILs and other organic molecules.⁷⁸

In summary, we chose a nonpolarizable UA force field to make it computationally effective. The average polarization effect was accounted for by the reduced ion charges by fitting the ESP of ion pair dimer. As a compromise between transferability and accuracy, a few simplifications were carefully chosen and applied to the proposed force field.

2.2. Functional Form. The classical functional form of the force field in AMBER/OPLS style was used as follows³⁸

$$\begin{aligned} U = & \sum_{\text{bonds}} K_r(r - r_0)^2 + \sum_{\text{angles}} K_\theta(\theta - \theta_0)^2 \\ & + \sum_{\text{dihedrals}} K_\chi[1 + \cos(n\chi - \delta)] \\ & + \sum_{i < j} 4\epsilon_{ij} \left[\left(\frac{\sigma_{ij}}{r_{ij}} \right)^{12} - \left(\frac{\sigma_{ij}}{r_{ij}} \right)^6 \right] + \sum_{i < j} \frac{q_i q_j}{r_{ij}} \quad (1) \end{aligned}$$

where K_r , K_θ , and K_χ are energy coefficients of the bonds, angles, and dihedrals, respectively, ϵ_{ij} and σ_{ij} are the energy and size parameters between atoms i and j in the Lennard-Jones (LJ) potential, and q_i is the charge on atom i . The cross parameters for interactions between unlike atoms are obtained by using the Lorentz-Berthelot (LB) combining rules. A scaling factor of 0.5 is applied to both of the LJ and Coulombic interactions between atoms separated by three consecutive bonds (1–4 interactions).⁷¹

2.3. Atom Partial Charges Assignment. Although the polarization is not included explicitly in the present force field, the averaged effect of polarization is accounted for by the effective atom partial charges. As in our previous work,⁷¹ we used ab initio calculations of ion pair dimers to fit the atom partial charges by the RESP method.⁷² The ion pair dimer is a much better choice to mimic the ESP around the ion in the bulk phase than an isolated ion or a single ion pair.⁷⁹ It is also affordable in terms of computational cost.

The ion pair dimers were optimized at the B3LYP/6-31+G(d,p) level using the Gaussian03 packages.⁸⁰ Additional vibration analysis was carried out to ensure the absence of negative frequencies and verify the existence of a true minimum. The ESP was generated by the Merz-Kollman (MK) method at the B3LYP/cc-pVTZ level, followed by a two-stage RESP fitting.⁷² All atom charges were optimized at the first

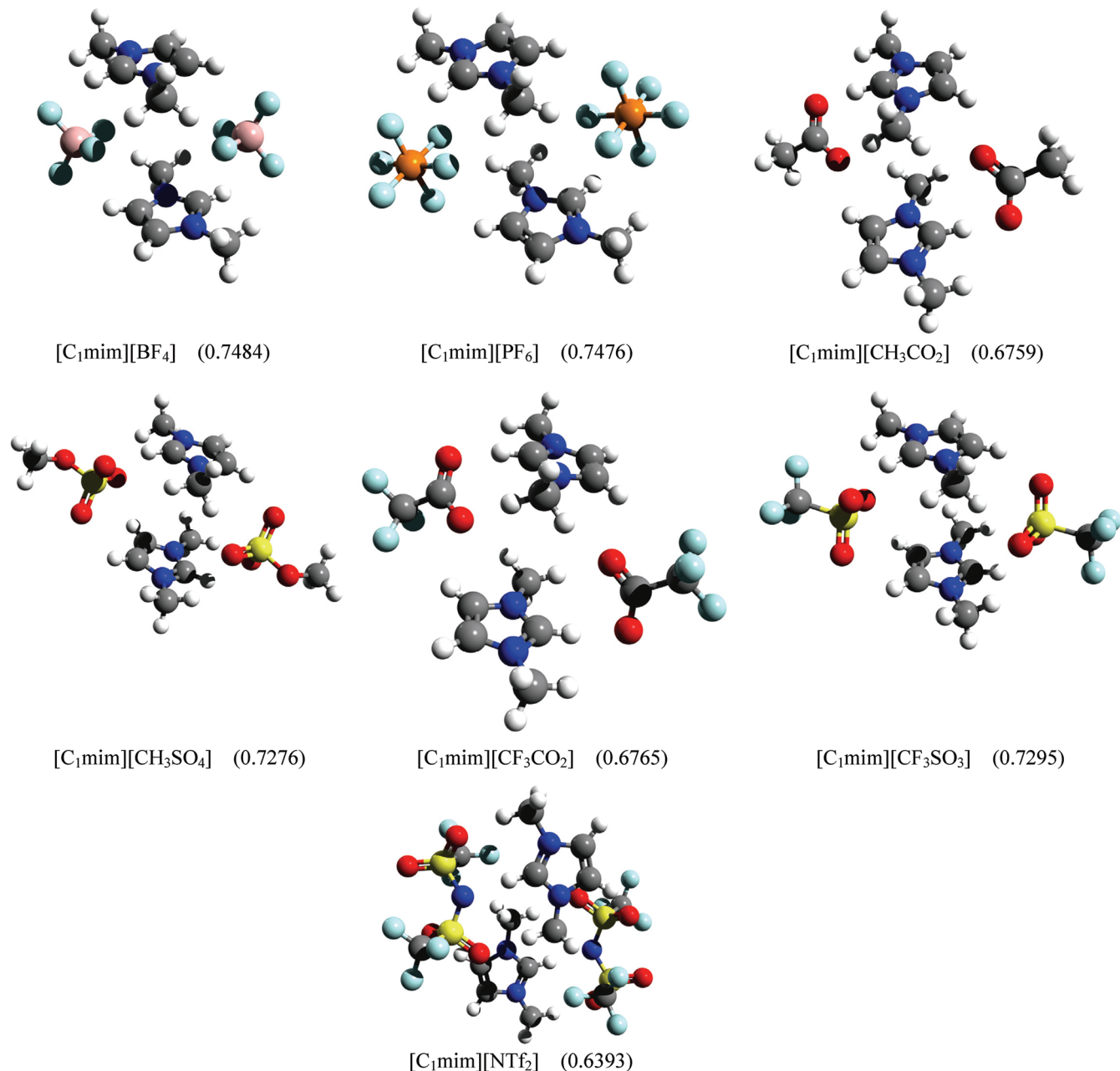


Figure 2. Optimized geometry of ion pair dimers $[\text{C}_1\text{mim}][\text{X}]$ by ab initio calculations at the B3LYP/6-31+G(d,p) level. The total charges on anions (e) are shown as the numbers in parentheses. Their x,y,z coordinates are given in the Supporting Information.

stage, and the charges on equivalent atoms (for example, the same type atom in the ion pair dimer) were restricted to be the same at the second stage. The restraint weight factors were chosen as 0.005 and 0.001 at the two stages, respectively. Because the groups of CH₂, CH₃, and CF₃ were treated as UA, the F and H atoms in these groups were not included in the fitting procedure. Instead, the center of mass (COM) of the UA group was used in the fitting.³⁹

Seven kinds of ion pair dimers were optimized in this work, including $[\text{C}_1\text{mim}]^+$ cation combined with $[\text{BF}_4]^-$, $[\text{PF}_6]^-$, $[\text{CH}_3\text{CO}_2]^-$, $[\text{CH}_3\text{SO}_4]^-$, $[\text{CF}_3\text{CO}_2]^-$, $[\text{CF}_3\text{SO}_3]^-$, and $[\text{NTf}_2]^-$ anions. The structures are shown in Figure 2 (their x,y,z coordinates can be found in the Supporting Information). A few conformers could be obtained by optimization from different

starting structures, which represent the local minimum of the ion pair dimers. However, it is beyond the scope of the present work to explore these conformers. As shown in Figure 2, the conformers in which the two imidazolium rings are parallel stacked were chosen to fit the charges. Another common characteristic feature of these conformers is that each anion was ‘shared’ by the H5 (see Figure 1) side of one cation and H4 side of the other cation. This may be the best choice among ion pair dimers to mimic the chemical environment around an ion in the bulk phase.

To obtain the optimized ion pair dimers in Figure 2, we built the initial configurations by replacing the chloride in our previous optimized $[\text{C}_1\text{mim}][\text{Cl}]$ dimer by more complicated anions. It is not trivial to optimize an ion pair dimer as complicated as

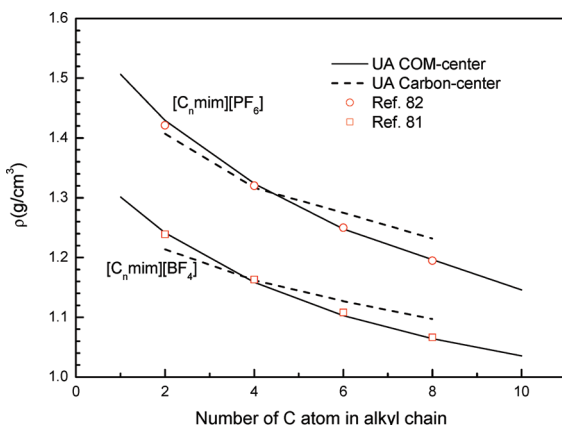


Figure 3. Simulated liquids densities (lines) of $[C_n\text{mim}][\text{BF}_4]$ and $[C_n\text{mim}][\text{PF}_6]$ at 353 K as a function of alkyl chain length (n) in cations compared to experimental data (Dots): (solid line) molecular dynamics (MD) results in this work by the force field using the center of mass (COM) of CH_3/CH_2 as the center of the UA group; (dotted line) MD results in this work by the force field using the carbon center as the center of the UA group.

$[\text{C}_1\text{mim}][\text{NTf}_2]$. In the case that an optimized structure without the above two features was obtained, the procedure has to be tried again with a slightly different initial configuration, which can be obtained by optimization at a relatively low level method such as AM1.

The total charges (absolute values) of the anions, which reflect the charge transfer between the cations and anions, are 0.7484, 0.7476, 0.6759, 0.7276, 0.6765, 0.7295, and 0.6393 for $[\text{BF}_4]^-$, $[\text{PF}_6]^-$, $[\text{CH}_3\text{CO}_2]^-$, $[\text{CH}_3\text{SO}_4]^-$, $[\text{CF}_3\text{CO}_2]^-$, $[\text{CF}_3\text{SO}_3]^-$, and $[\text{NTf}_2]^-$, respectively. The value was compared with 0.7046 for the $[\text{C}_1\text{mim}]\text{Cl}$ dimer, as reported in our previous work.⁷¹

As mentioned in section 2.1, the RESP charges were scaled to 0.8e to obtain a transferable force field for different ILs. Although the value of 0.8 is just an empirical correction to achieve transferability of the force field, which does not describe the different polarizabilities in different ILs, it gives good performance for all the ILs studied in this work (see section 4). Of course, the atom partial charges on the $[\text{C}_1\text{mim}]^+$ cation are still different after scaling. However, the difference is within 0.05e for the eight ILs studied. Thus, the atom partial charges on the cation were adopted as the same in our previous work.⁷¹ The charges of both the cations and the anions are listed in Table S1 in the Supporting Information.

2.4. Bond and Angle Parameters. Usually the carbon atom was adopted as the center of the pseudo-UA group in the UA force field. Thus, the equilibrium bond lengths and angles in the AA model can be used. However, the center of mass (COM) of the UA group does not essentially locate at the carbon center. For example, the COM of CH_3 deviates about 0.07 Å from the carbon atom, while that of CF_3 deviates about 0.37 Å. We found it was difficult to reproduce the liquid densities of all the ILs studied in this work if the carbon atom was chosen as the center of UA. As shown in Figure 3, the density of $[\text{C}_4\text{mim}][\text{BF}_4]$ is well predicted when the carbon-centered UA was used. However, the densities of $[\text{C}_n\text{mim}][\text{BF}_4]$ are underestimated when $n < 4$ while overestimated when $n > 4$. A similar trend is also observed for ILs of the $[\text{C}_n\text{mim}][\text{PF}_6]$ family. Prediction of the densities is significantly improved when the COM of the UA group is adopted as the center. The results of $[\text{C}_n\text{mim}][\text{BF}_4]$

and $[\text{C}_n\text{mim}][\text{PF}_6]$ are in very good agreement with experiments^{81,82} (see Figure 3). It was also reported in another classical UA force field that use of an off-carbon-center UA group would improve the performance of the model. For example, van Gunsteren and co-workers⁸³ showed that better agreement with experimental data was obtained when the bond length of CH_3-O was 0.1 Å larger than that of C–O in their 3-site model of methanol.

In this work, we used the coarse-grain (CG) method developed by Klein and co-workers⁸⁴ to obtain the bond and angle parameters of the UA groups. The central idea of the method is to mimic structural properties obtained from simulations by the corresponding AA model.

First, a primary AA force field was constructed by extraction of the force constants from AMBER-GAFF,⁷⁷ while the equilibrium bond lengths and angles were determined in aims of the ab initio calculations and XRD experiments. Second, molecular dynamics simulations by the AA model were performed with 100 ion pairs in the NpT ensemble at 298.15 K and 1 atm. The probability distributions of the bonds and angles were collected in terms of the COM of UA groups. Then, the bond lengths r_0 and force constants K_r were adjusted and optimized by a few UA simulations until the mean and variance of the distributions were reproduced. The equilibrium angle θ_0 and force constants K_θ were determined in a similar way. Comparisons between the bond and the angle distributions obtained from AA and UA simulations are shown in Figures S1 and S2 in the Supporting Information, respectively. The values of r_0 , K_r and θ_0 , K_θ are also listed in Table S1 in the Supporting Information.

2.5. Lennard-Jones Parameters. As shown in Figure 1, five UA types were defined in this work, i.e., CT2, CT3, CN2, CN3, and CF3. Among them, CN3/CN2 are slightly different from CT3/CT2 because the carbon is attached to an electron-withdrawing atom, such as N and O, resulting in the type of hydrogen in the AMBER force field being slightly different.

In this work, we adopted the LJ parameters of CT3/CT2 in the transferable potentials for phase equilibria (TraPPE) developed by the Siepmann group.⁸⁵ The well depth ϵ of CN3/CN2 was set to be the same as that of CT3/CT2, while the size parameter (σ) was obtained by scaling between the TraPPE and our previous parameters.³⁹

The LJ parameters of CF3 were obtained by a similar mapping method in section 2.4, while the target function used was the site–site radial distribution functions (RDFs) of CF_3-CF_3 . The RDF was obtained by simulating the saturated liquid hexafluoroethane (C_2F_6) at 200 K by the AA force field. Then, the LJ parameters in the UA were adjusted until the RDF was matched to the results by AA, as shown in Figure S3 in the Supporting Information. The final parameters of the CF3 in this work (see Table S1 in the Supporting Information) are very close to those developed by Cui et al.,⁸⁶ with a slightly smaller diameter.

The H atoms on the imidazolium ring (H4 and H5) were not included in any UA groups, because they incline to form hydrogen bonds with the anions. Their LJ parameters were also adjusted to match the optimized geometries of isolated ion pairs in our previous work.^{38,39} In this work, we adopted the LJ parameters of H4 and H5 obtained by $[\text{C}_1\text{mim}][\text{Cl}]$ ion pairs, which is developed in our recent work.⁷¹

2.6. Dihedral Angle Parametrization. The dihedral terms in eq 1, usually described by a cosine series, are used to reproduce the torsion energy profiles of the corresponding dihedrals. The dihedral coefficients were optimized to fit the torsion energy

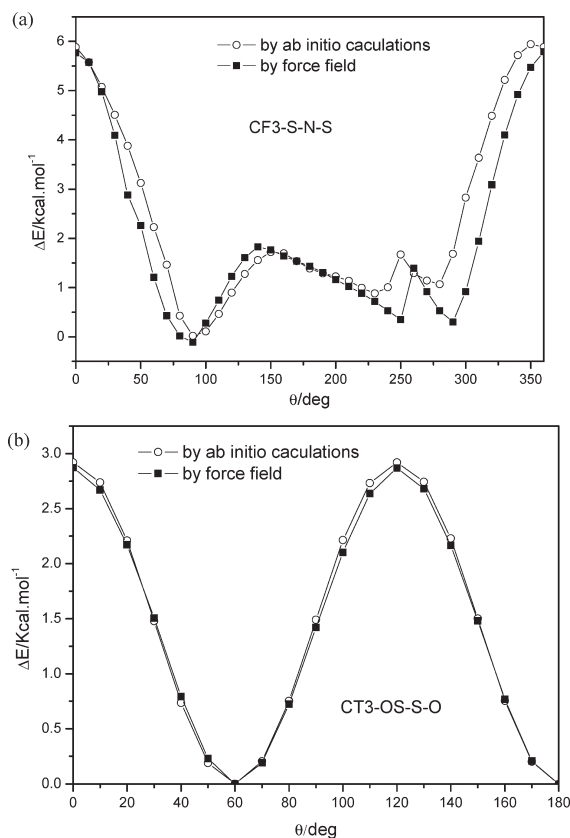


Figure 4. Dihedral energy profiles of $[\text{Tf}_2\text{N}]^-$ (a) and $[\text{CH}_3\text{SO}_4]^-$ (b) obtained by ab initio calculations at the MP2/cc-pVTZ//B3LYP/6-31+G(d,p) level (QM, open circles) and the optimized force field in this work (MM, solid squares).

profiles obtained by ab initio calculations at the MP2/cc-pVTZ//B3LYP/6-31+G(d,p) level. The detailed fitting procedure was described in our previous work.⁷¹

The coefficients of two dihedrals, i.e., CT3–OS–S–O in $[\text{CH}_3\text{SO}_4]^-$ and CF3–S–N–S in $[\text{NTf}_2]^-$ (see Figure 1 for their schematic structures), were fitted in this work. As shown in Figure 4, the agreement between the ab initio calculations and those obtained from the force field is fairly good.

As mentioned above, the UA model in TraPPE was used in this work to describe the alkyl groups. However, the scaling factor of the 1–4 interactions used in TraPPE is zero,⁸⁵ which is quite different from the value of 0.5 in this work. Thus, the dihedral coefficients (X–CT2–CT2–X) were refitted to correctly describe the internal rotation of alkyl groups, which are different from the values in TraPPE.⁸⁵

All of the final optimized parameters of the force field can be found in Table S1 in the Supporting Information.

3. SIMULATION DETAILS

All molecular dynamics simulations were carried out using the parallel LAMMPS package.⁸⁷ The simulated system included typically 150 ion pairs, while a few larger systems (400 ion pairs) were also simulated, and no significant difference was found for the reported properties in this work. The initial configuration was prepared by PACKMOL⁸⁸ in a cubic box, typically larger than its “real” size to make the packing easier, followed by a conjugate gradient energy minimization within

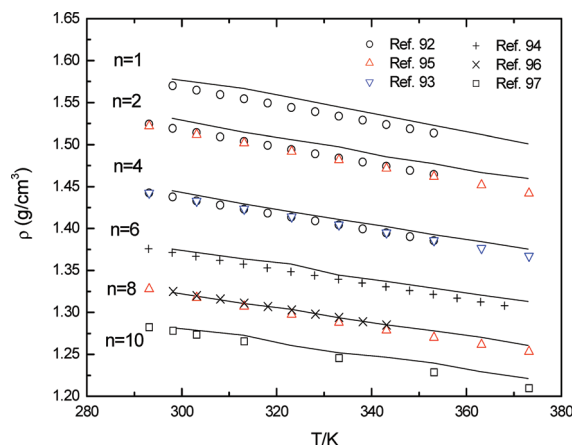


Figure 5. Simulated liquid densities (line) of ionic liquids $[\text{C}_n\text{mim}][\text{Tf}_2\text{N}]$ as a function of temperature. Experimental values are shown as open symbols.

1000 steps. Due to the slow dynamics of ILs, the system was heated to 700 K in NpT ensemble for about 1 ns to overcome the possible energetic trapping. Then, the system was cooled (typically 50 K/10 000 steps) to the target temperature, followed by 3 ns equilibrium NpT simulation. Another 4 ns NpT run was performed to obtain the ensemble-averaged intermolecular energies and liquid densities.

After the averaged box size was obtained, MD simulations in NVT ensembles were carried out to calculate the viscosity and self-diffusion coefficients. The equilibrated period lasted about 10 ns, leading to the system pressure about 0.1 MPa. In this work, the viscosity was calculated via equilibrium MD simulations (see section 4.4 for details). The simulations were carried out long enough (typically 20–60 ns) to obtain better statistical sampling. The nine components of the pressure tensors were recorded at every time step, and multiple time origin average method were used to improve the statistics.^{71,89} The atom coordinates were stored every 4 ps for postanalysis.

All simulations were performed in a time step of 2 fs. Periodic boundary conditions were employed in three dimensions. The temperature and pressure were controlled by a Nose–Hoover thermostat and barostat, with update frequencies of 0.2 and 2 ps, respectively. All bonds and angles related to hydrogen were held rigid using the SHAKE algorithm with a tolerance of 10^{-4} and maximum iterations of 10. A cutoff of 1.2 nm was set for both the LJ and the Coulombic interactions. The LJ tail correction was added to the energy and pressure, and the long-range electrostatic interactions were dealt with using the particle–particle particle mesh (PPPM) solver. The neighbor lists were built with a skin distance of 0.2 nm every 5 steps.

4. RESULTS AND DISCUSSION

At the meeting of IUPAC project 2002-005-1-100, the IL $[\text{C}_6\text{mim}][\text{NTf}_2]$ was designated as the reference material (IUPAC standard IL) for testing measurement techniques,⁹⁰ because it is stable, has low water solubility, and is easily prepared and purified. In addition, the recommended values of its properties were also published^{90,91} and provide a good source to validate the force field proposed here. Therefore, we focus on the properties of $[\text{C}_n\text{mim}][\text{NTf}_2]$ ($n = 1, 2, 4, 6, 8, 10$) in this work. For other anions, only ILs with $[\text{C}_4\text{mim}]^+$ were simulated.

Table 1. Simulated Densities (in g/cm³) of Ionic Liquids by the Force Field Proposed in This Work

ionic liquid	298 K	313 K	323 K	333 K	343 K	353 K	363 K	373 K
[C ₁ mim][NTf ₂]	1.578	1.567	1.556	1.545	1.534	1.523	1.512	1.501
[C ₂ mim][NTf ₂]	1.531	1.514	1.506	1.497	1.485	1.477	1.467	1.459
[C ₄ mim][NTf ₂]	1.445	1.429	1.420	1.411	1.402	1.392	1.384	1.375
[C ₆ mim][NTf ₂]	1.375	1.364	1.357	1.344	1.337	1.329	1.320	1.313
[C ₈ mim][NTf ₂]	1.324	1.310	1.303	1.293	1.285	1.278	1.270	1.260
[C ₁₀ mim][NTf ₂]	1.282	1.272	1.260	1.252	1.247	1.240	1.229	1.221
[C ₄ mim][CF ₃ SO ₃]	1.320	1.309	1.301	1.293	1.285	1.276	1.268	1.261
[C ₄ mim][CF ₃ CO ₂]	1.212	1.205	1.199	1.191	1.183	1.176	1.168	1.161
[C ₄ mim][CH ₃ CO ₂]	1.055	1.046	1.040	1.032	1.028	1.022	1.016	1.011
[C ₄ mim][CH ₃ SO ₄]	1.235	1.226	1.222	1.213	1.208	1.200	1.196	1.190
[C ₄ mim][PF ₆]	1.370	1.357	1.347	1.338	1.328	1.324	1.313	1.304
[C ₄ mim][BF ₄]	1.196	1.187	1.180	1.173	1.165	1.158	1.150	1.143

4.1. Liquid Densities. The liquid densities of ILs of the [C_nmim][NTf₂] family were predicted using the force field at ambient pressure and eight temperatures ranging from 298 to 373 K. As shown in Figure 5, the simulated densities are in very good agreement with the experimental values.^{92–97} The largest deviation between simulations and experiments is within 0.7%. In the case of [C₆mim][NTf₂], the temperature dependence of densities (ρ) can be given by a linear fitting

$$\rho / (\text{kg} \cdot \text{m}^{-3}) = 1630.7 \pm 7.5 - 0.854 \pm 0.022(T / \text{K}) \quad (2)$$

which is very close to the recommended equation⁹¹ derived from experiments

$$\rho / (\text{kg} \cdot \text{m}^{-3}) = 1640.95 - 0.9012(T / \text{K}) \quad (3)$$

The isobaric thermal expansion coefficients can also be estimated through the above equations. The simulated value was $6.2 \times 10^{-4} \text{ K}^{-1}$, about 5% smaller than that by experiments, $6.57 \times 10^{-4} \text{ K}^{-1}$.

The simulated densities of ILs with the other six anions in combination with [C₄mim]⁺ are also listed in Table 1. The liquid densities are predicted very well by MD simulations in the temperature range from 298 to 373 K, as shown in Figure 6. The deviations between simulations and experimental data^{95,98–102} are within 1% for [NTf₂]⁻, [CF₃CO₂]⁻, [CH₃CO₂]⁻, [PF₆]⁻, and [BF₄]⁻-based ILs, while for [CF₃SO₃]⁻ and [CH₃SO₄]⁻-based ILs, the deviations are 1.3% and 2.1%, respectively.^{100,101,103}

4.2. Enthalpies of Vaporization. The enthalpies of vaporization, ΔH^{vap} , are a valuable experimental source in developing and validating force fields.¹⁰⁴ However, in the case of ILs, measurement of vapor–liquid equilibrium properties is extremely difficult, due to the competition between vaporization and thermal decomposition as well as the impurities in IL samples.¹⁰⁵ Fortunately, some promising progress was made recently, especially for the [C_nmim][NTf₂] family, due to their good thermal stability at temperatures as high as 600 K. The enthalpies of vaporization of [C_nmim][NTf₂] were measured by a variety of methods such as Knudsen effusion,¹⁰⁶ surface tension,¹⁰⁶ microcalorimetry,¹⁰⁷ mass spectrometrically detected temperature-programmed desorption (TPD),¹⁰⁸ transpiration,¹⁰⁹ and a thermogravimetric approach.¹¹⁰

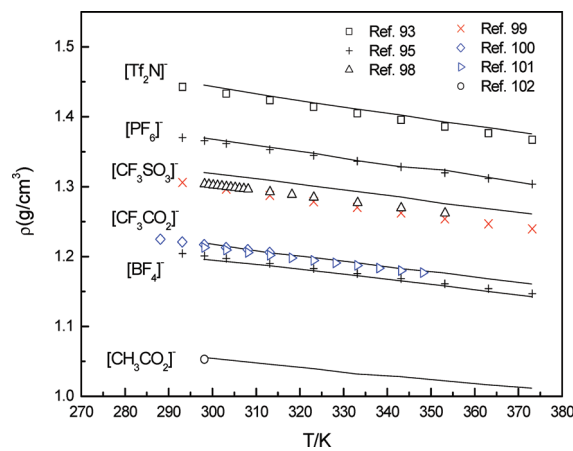


Figure 6. Simulated liquid densities (line) of ionic liquids [C₄mim][X] as a function of temperature. Experimental values are shown as open symbols.

In simulations, ΔH^{vap} is calculated from the difference between the molar internal energy of the gas (U^{gas}) and liquid (U^{liq}) phases using eq 4³⁸

$$\Delta H^{\text{vap}} = RT - (U^{\text{liq}} - U^{\text{gas}}) \quad (4)$$

where R is the gas constant. The gas phase is simulated by an isolated ion pair at the same temperature in a large enough box and no cutoffs and long-range corrections were applied.³⁹

The simulated values of ΔH^{vap} at 298 K using the force field in this work for [C_nmim][NTf₂] are shown in Table 2. The results by various experimental methods were also listed for comparison as well as the simulation results by other force fields.^{107,111–114} As shown in Figure 7, good agreement was found between the simulations in this work and experimental measurements, except for the microcalorimetric data. For example, the enthalpies of vaporization for [C₂mim][NTf₂] were measured between the values of 134 and 141 kJ/mol, a reasonable range comparable to the uncertainties in experiments (e.g., ± 3 kJ/mol for TPD¹⁰⁸ and thermogravimetry¹¹⁰ and ± 6 kJ/mol for calorimetry¹⁰⁷). We obtained a value of 138.1 kJ/mol, in good agreement with the experiments. The classical (nonpolarizable) force field without scaling the charges tend to overestimate ΔH^{vap} with values of 146 kJ/mol by a CHRAMM-derived force field (hereinafter referred to as

Table 2. Estimated Values of Enthalpies of Vaporization, $\Delta H^{\text{vap}}(298\text{K})$ in kJ/mol, of Ionic Liquids $[\text{C}_n\text{mim}][\text{NTf}_2]$ by Various Experimental Methods, Compared with Simulation Results by Different Force Fields

n	experiments					MD simulations					
	Knudsen ¹⁰⁶	TPD ¹⁰⁸	gravimetry ¹¹⁰	microcalorimetry ¹⁰⁷	transpiration ¹⁰⁹	this work	Maginn ¹¹²	Ludwig ⁶⁹	Borodin ¹¹³	Santos ¹⁰⁷	Shimizu ¹¹⁴
1						139.7		132.1			
2	135.3	134	141	136	136.7	138.1	146	130.6	127.7	159	173
4	136.2	134	139	155		142.2	151	135.1	133.7	174	180
6	139.8	139	145	173		148.5	157	143.8	141.9	184	185
8	150.0	149	153	192		156.8	162	153.6		201	189
10			155			162.6					

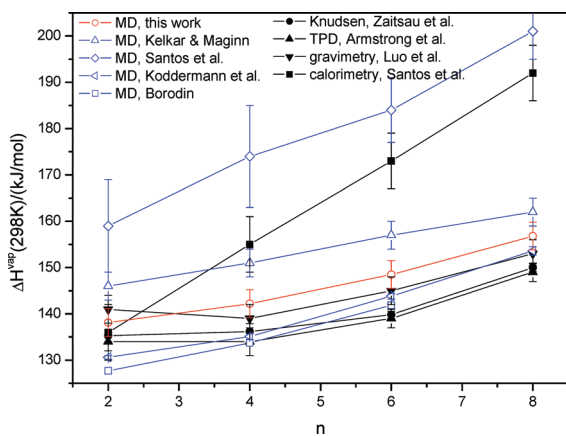


Figure 7. Heats of vaporization for $[\text{C}_n\text{mim}][\text{NTf}_2]$ at 298 K versus alkyl chain length measured by various experimental methods (solid symbols) including microcalorimetry, Knudsen, TPD, and gravimetry. Predicted values by molecular dynamics (MD) simulations are shown as open symbols, with different force fields proposed by Santos et al., Koddermann et al., Lopes and Padua, Kelkar and Maginn, Borodin, and this work.

Maginn),¹¹² 159 and 173 kJ/mol by a OPLS-ABMER-based force field (hereinafter referred to as Santos¹⁰⁷ and Shimizu,¹¹⁴ respectively). However, the refined classical force field proposed by Köddermann et al. (hereinafter referred to as Ludwig)⁶⁹ performed quite well, giving a value of 130.6 kJ/mol, by the adjustments of LJ parameters. A slightly lower value of 127.7 kJ/mol was predicted by the polarizable force field proposed by Borodin (hereinafter referred to as Borodin).¹¹³

All simulations predicted a nearly linear increase of ΔH^{vap} with the increase of alkyl chain length on the cations, which is in line with the experiments when $n > 4$. For shorter chains ($n < 4$), the measured chain length has much less influence on the value of ΔH^{vap} than that in simulations. For example, the ΔH^{vap} of $[\text{C}_4\text{mim}][\text{NTf}_2]$ is essentially the same as (or even lower than) that of $[\text{C}_2\text{mim}][\text{NTf}_2]$ by Knudsen, TPD, and gravimetric measurements. However, the simulations did predict a bit lower value of ΔH^{vap} for $[\text{C}_2\text{mim}][\text{NTf}_2]$ compared to $[\text{C}_1\text{mim}][\text{NTf}_2]$, indicating the observed trend in experiments. The force field in this work predicted the enthalpy of vaporization increases by about 3.7 kJ/mol per CH_2 group, in excellent agreement with the experimental values of 3.5 (Knudsen),¹⁰⁶ 3.8 (TPD),¹⁰⁸ and 3.5 kJ/mol (gravimetry),¹¹⁰ which is comparable with the simulated results of Ludwig (4.6 kJ/mol),¹¹¹ and Borodin (4.1 kJ/mol).¹¹³ A bit weaker increase of ΔH^{vap}

Table 3. Estimated Enthalpies of Vaporization, ΔH^{vap} (500K) in kJ/mol, and Averaged Values of ΔC_p (in J/(K·mol)) Calculated in the Temperature Range from 298 to 500 K of Ionic Liquids $[\text{C}_n\text{mim}][\text{NTf}_2]$ by Various Experimental Methods

n	experiments						
	simulations, this work		ΔH^{vap} (500K)		ΔC_p^a		
	ΔH^{vap} (500 K)	ΔC_p^a	Knudsen ¹⁰⁶	TPD ¹⁰⁸	gravimetry ¹¹⁰	I ^b	
1	123.4	81					
2	121.3	83	115	115	120	90.7	116
4	124.6	87	116	115	118	95.5	125
6	127.6	104	120	120	124	100.3	137
8	133.3	116	130	130	133	105.0	148
10	139.6	114				135	

^a The average difference between the molar heat capacity at constant pressure of the gas and that of the liquid. ^b Estimated using the energy equipartition principle and thermodynamic relationships (details in the Supporting Information of ref 107). ^c Calculated from the measured molar heat capacity of the liquids¹¹⁵ and ab initio calculation results of the ideal gases.¹¹⁶

per CH_2 group was predicted by the force fields of Shimizu (2.3 kJ/mol)⁹¹ and Maginn (2.8 kJ/mol),¹¹² while a higher value of increase of ΔH^{vap} per CH_2 was given by Santos (6.8 kJ/mol).¹⁰⁷ The microcalorimetric measurements gave an even stronger increase (9.2 kJ/mol)¹⁰⁷ of ΔH^{vap} per CH_2 group.

It should be noted that the above experimental values of ΔH^{vap} were not measured directly at room temperature (298 K). Instead, most of them were obtained at a higher average temperature, typically 500 K, by the linear fitting of the temperature-dependent properties of ILs.¹⁰⁵ Then the enthalpy of vaporization at 298 K was acquired by an estimated value of ΔC_p , the average difference between the molar heat capacity at constant pressure of the gas and that of liquid. In most cases,^{105,106,109} a value of 100 J/(K·mol) was used for all of the ILs studied.

In this work, we also simulated ΔH^{vap} at 500 K to make comparisons with experiments. The value of ΔC_p was also obtained, as shown in Table 3. The simulated ΔH^{vap} of $[\text{C}_n\text{mim}][\text{NTf}_2]$ at 500 K in this work agreed well with those by experiments. The overestimation of about 5 kJ/mol was in the range of uncertainties of both experiments and simulations. The simulated values of ΔC_p for $[\text{C}_n\text{mim}][\text{NTf}_2]$ family

Table 4. Estimated Values of Enthalpies of Vaporization, ΔH^{vap} in kJ/mol, of Ionic Liquids by Spectrometrically Detected Temperature-Programmed Desorption (TPD) Experiments, Compared with Simulation Results by the Force Fields in This Work

ionic liquid	simulations			experiments ¹⁰⁸	
	ΔH^{vap}		ΔC_p	ΔH^{vap}	
	298K	500K		298K	500K
[C ₄ mim][CF ₃ SO ₃]	150.7	134.7	79		
[C ₈ mim][CF ₃ SO ₃]	165.0	143.3	107	151	132
[C ₄ mim][PF ₆]	152.9	135.1	88		
[C ₈ mim][PF ₆]	166.7	144.7	109	169	150
[C ₂ mim][BF ₄]	142.8	128.5	71		
[C ₄ mim][BF ₄]	144.3	128.5	78		
[C ₈ mim][BF ₄]	158.0	139.1	94	162	143
[C ₄ mim][CF ₃ CO ₂]	140.2	123.6	82		
[C ₄ mim][CH ₃ CO ₂]	150.2	131.2	94		
[C ₄ mim][CH ₃ SO ₄]	173.9	155.4	92		

Table 5. Self-Diffusion Coefficients (10^{-7} cm²/s) of Ions in Ionic Liquids at 353 K, Obtained from Simulations in This Work and Compared to Experimental Values

ionic liquid	simulations		experiments ¹⁰⁰	
	cation	anion	cation	anion
[C ₁ mim][NTf ₂]	17.9	8.9	22	13
[C ₂ mim][NTf ₂]	18.5	10.2	22	14
[C ₄ mim][NTf ₂]	10.9	7.8	15	13
[C ₆ mim][NTf ₂]	6.9	6.2	12	11
[C ₈ mim][NTf ₂]	4.0	4.0	9.0	8.8
[C ₁₀ mim][NTf ₂]	2.2	2.6		
[C ₄ mim][CF ₃ SO ₃]	7.8	6.0	10	9.0
[C ₄ mim][CF ₃ CO ₂]	19.8	17.2	12	11
[C ₄ mim][PF ₆]	4.7	3.2	6.7	5.7
[C ₄ mim][BF ₄]	9.7	8.2	11	11
[C ₄ mim][CH ₃ CO ₂] ^a	3.5	3.2		
[C ₄ mim][CH ₃ SO ₄] ^a	1.39	0.88		

^a Self-diffusion coefficients at 343 K.

were in the range of 80–120 J/(K·mol), which is also comparable with those derived from different experimental sources.^{107,115,116}

Table 4 summarizes MD-simulated values of ΔH^{vap} for other ILs at 298 and 500 K as well as a few available experimental data via the TPD method.¹⁰⁸ Our force field predicted ΔH^{vap} for [C₈mim][BF₄] of 158.0 and 139.1 kJ/mol at 298 and 500 K, respectively, which is in good agreement with those obtained by TPD measurements (162 and 143 kJ/mol).¹⁰⁸ The predictions of ΔH^{vap} for [C₂mim][BF₄] and [C₄mim][BF₄] of 142.8 and 144.3 kJ/mol at 298 K are slightly higher than those obtained by Borodin's polarizable force field (135.3 and 140.8 kJ/mol). The results for [C₈mim][PF₆]¹⁰⁸ were also in good agreement with TPD measurements,¹⁰⁸ while the values of ΔH^{vap} for [C₈mim][CF₃SO₃]¹⁰⁸ were about 10% larger than the TPD experimental values.¹⁰⁸

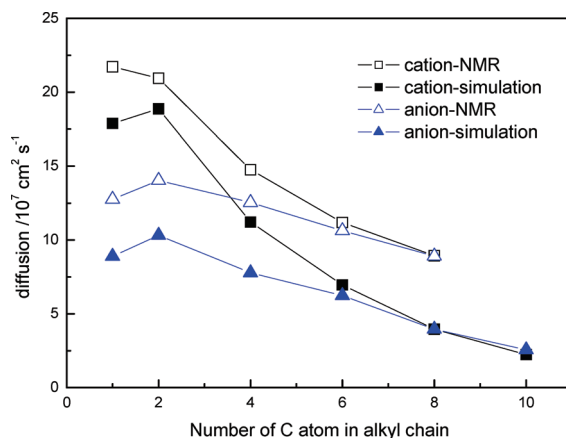


Figure 8. Alkyl chain length dependence of self-diffusion coefficients for ionic liquids [C_nmim][NTf₂] at 353 K. Simulated values (solid symbols) in this work are compared with experimental measurements (open symbols) by the pulsed-field-gradient spin echo (PGSE) NMR method.

In summary, the force field proposed in this work predicts the enthalpies of vaporization with good accuracy as well as their dependence on the temperature and alkyl chain length of the cations.

4.3. Self-Diffusion Coefficient. Unlike the liquid densities, the transport properties are very sensitive to the parameters of the force field.^{48,117} Thus, it is a more critical validation by comparing the results of the transport coefficients between simulations and experiments, such as the self-diffusion coefficient and zero-shear viscosity.

The self-diffusion coefficient D_i for species i was calculated using the Einstein relation

$$D_i = \frac{1}{6} \lim_{t \rightarrow \infty} \frac{d}{dt} \langle [\vec{r}_i(t) - \vec{r}_i(0)]^2 \rangle = \frac{1}{6} \lim_{t \rightarrow \infty} \frac{d\Delta r_i^2}{dt} \quad (5)$$

where the quantity in $\langle \dots \rangle$ is the ensemble-averaged mean square displacement (MSD) of the COM of the cations or anions. As mentioned in our previous work,⁷¹ it needs a rather long MD trajectory to obtain a reliable value of the self-diffusion coefficient because of the slow dynamics of ILs. In this work, the self-diffusion coefficient was determined by linear fitting of the 4–10 ns slope of MSD in each case, which was calculated from more than 20 ns MD trajectories. As shown in Figure S4 in the Supporting Information, although the calculated $\beta(t) = (d\log\Delta r_i^2(t))/(d\log(t))$ cannot approach 1.0 at 298 K, the linear fitting of the 4–10 ns slope of the MSD can give a reliable estimation of the self-diffusion coefficient. At 373 K, the value of β approached 1.0 when $t > 2$ ns. A more detailed discussion can be found in our previous work.⁷¹

The simulated D_i of ions of 12 ILs at 353 K are summarized in Table 5 and compared with the available experimental values measured by the pulsed-field-gradient spin echo (PGSE) NMR method.^{118,119} For [C_nmim][NTf₂] family ILs, the force field slightly underestimates the self-diffusion coefficients of both ions in [C_nmim][NTf₂], as shown in Figure 8. The relative deviation between simulation and experiment increases with the alkyl chain length. The predicted D_i of both ions in [C₈mim][NTf₂] is 4.0×10^{-7} cm²/s, while the value in experiment is 8.9×10^{-7} cm²/s. Similar results were reported by Köddermann et al.⁹⁷ for their refined force field. In addition,

Table 6. Temperature-Dependent Self-Diffusion Coefficients (in $10^{-7} \text{ cm}^2/\text{s}$) of Ions in Ionic Liquid $[\text{C}_n\text{mim}][\text{NTf}_2]$, Obtained from Simulations in This Work and Compared to Experimental Values

<i>T</i>	simulations		experiments ¹¹⁹	
	cation	anion	cation	anion
298	0.67	0.51	1.68	1.52
313	1.33	1.05	3.21	2.96
323	2.36	1.87	4.6	4.3
333	3.3	2.5	6.4	6.0
343	5.5	3.9	8.6	8.1
353	6.9	6.2	11.2	10.6
363	9.5	7.7	14.2	13.5
373	12.3	10.5	17.6	16.9

two of the features about the diffusion of the $[\text{C}_n\text{mim}][\text{NTf}_2]$ series ILs were also well reproduced: (1) The dependence of D_i on the alkyl chain length in the imidazolium cations is predicted in the same order as that in the NMR experiments:¹¹⁹ $[\text{C}_2\text{mim}][\text{NTf}_2] > [\text{C}_1\text{mim}][\text{NTf}_2] > [\text{C}_4\text{mim}][\text{NTf}_2] > [\text{C}_6\text{mim}][\text{NTf}_2] > [\text{C}_8\text{mim}][\text{NTf}_2]$, as shown in Figure 8. The result is also consistent with the predicted values of ΔH^{vap} in Table 2, in which $[\text{C}_2\text{mim}][\text{NTf}_2]$ has the lowest value of ΔH^{vap} , indicating the increase of ΔH^{vap} leads to slower dynamics of ILs. (2) The cations move much faster than the anions in ILs $[\text{C}_2\text{mim}][\text{NTf}_2]$ and $[\text{C}_1\text{mim}][\text{NTf}_2]$, while the difference of D_i between the cations and anions becomes smaller and smaller with the increase of the alkyl chain length. Our force field predicts slightly faster dynamics of the anions in $[\text{C}_{10}\text{mim}][\text{NTf}_2]$ at 353 K. The ratios of the self-diffusion coefficients between the cations and anions D_+/D_- decreased from 2.0 to 1.0 when n increased from 1 to 8, compared with the experimental values of 1.8–1.0.

We also studied the temperature dependence of the self-diffusion coefficients of $[\text{C}_6\text{mim}][\text{NTf}_2]$ in the range from 298 to 373 K, as shown in Table 6. Although the simulated self-diffusion coefficients are underestimated about one-half or more, especially at lower temperature, all the values are in the same order of magnitude as those in experiments.¹¹⁹ It was also reproduced in simulations that the self-diffusion coefficients of the cations are about 10% larger than those of the anions.

The effects of anion species were evaluated by simulating the self-diffusion coefficients of the ions in the $[\text{C}_4\text{mim}]^+$ -based ILs, as shown in Table 6. In experiments, the following trend of the self-diffusion coefficients was found at 353 K:¹¹⁸ $[\text{C}_4\text{mim}][\text{NTf}_2] > [\text{C}_4\text{mim}][\text{CF}_3\text{CO}_2] > [\text{C}_4\text{mim}][\text{BF}_4^-] > [\text{C}_4\text{mim}][\text{CF}_3\text{SO}_3^-] > [\text{C}_4\text{mim}][\text{PF}_6^-]$. The trend was well reproduced by our force field, except the case of $[\text{C}_4\text{mim}][\text{CF}_3\text{CO}_2]$, in which the simulated values are about 50% overestimated. A similar trend was also found in the simulations reported by Tsuzuki et al.⁴²

4.4. Viscosities. Another crucial property describing the dynamic of ILs is the zero-shear viscosity, which can be calculated via equilibrium MD (EMD) using the Green–Kubo (GK) formula^{120,121}

$$\eta = \frac{V}{10k_B T} \int_0^\infty \left\langle \sum_{\alpha\beta} P_{\alpha\beta}(0) P_{\alpha\beta}(t) \right\rangle dt \quad (6)$$

Table 7. Simulated Viscosities (in $\text{mPa}\cdot\text{s}$) of Ionic Liquid Using the Force Field Developed in This Work Together with Experimental Values at 353 K

ionic liquids	simulations	experiments	ref
$[\text{C}_1\text{mim}][\text{NTf}_2]$	10.3	8.1	100
$[\text{C}_2\text{mim}][\text{NTf}_2]$	8.3	7.7	100
$[\text{C}_4\text{mim}][\text{NTf}_2]$	12.6	9.2	119
$[\text{C}_6\text{mim}][\text{NTf}_2]$	15.5	10.8	100
$[\text{C}_8\text{mim}][\text{NTf}_2]$	18.5	12.7	100
$[\text{C}_{10}\text{mim}][\text{NTf}_2]$	27.3	15.5	125
$[\text{C}_4\text{mim}][\text{CF}_3\text{SO}_3^-]$	17.3	13.0	100
$[\text{C}_4\text{mim}][\text{CF}_3\text{CO}_2]$	10.0	10.3	100
$[\text{C}_4\text{mim}][\text{PF}_6^-]$	39	22.8	100
$[\text{C}_4\text{mim}][\text{BF}_4^-]$	13	13.3	100
$[\text{C}_4\text{mim}][\text{CH}_3\text{CO}_2]$ ^a	50	42.0	126
$[\text{C}_4\text{mim}][\text{CH}_3\text{SO}_4]$ ^a	86	30.0	103

^a Viscosity at 343 K.

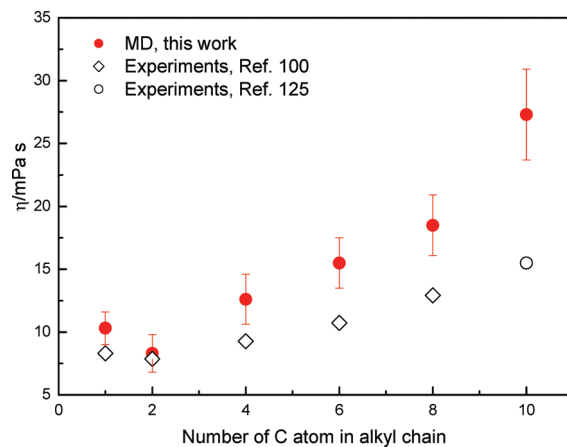


Figure 9. Alkyl chain length dependence of viscosities of ionic liquids $[\text{C}_n\text{mim}][\text{Tf}_2\text{N}]$. Simulated values in this work (solid circles) are compared with experimental measurements (open symbols).

The brackets indicate that the average must be taken over all time origins $t = 0$. V is the volume of the system, T is the temperature, and k is the Boltzmann constant. $P_{\alpha\beta}$ is the symmetrized traceless portion of the stress tensor $\sigma_{\alpha\beta}$. It is defined as

$$P_{\alpha\beta} = \frac{1}{2}(\sigma_{\alpha\beta} + \sigma_{\beta\alpha}) - \frac{1}{3}\delta_{\alpha\beta}\left(\sum_r \sigma_{rr}\right) \quad (7)$$

where $\delta_{\alpha\beta}$ is the Kronecker delta and $\delta_{\alpha\beta} = 1$ when $\alpha = \beta$; otherwise, $\delta_{\alpha\beta} = 0$. Note all nine components of the pressure tensor were used in eq 6 to improve the statistics. Unlike self-diffusion, the shear viscosity is a collective property, so it is not statistically improved by averaging over the number of particles in the system. The EMD-GK method is a direct and reliable tool for calculation of viscosity, and it was proved to give a reasonable estimation for the systems including ILs if long enough simulations (several tens of nanoseconds) were carried out.^{122–124} In this work, the pressure tensor information was recorded at every time step and a trajectory of 20–60 ns was

Table 8. Simulated Viscosities (in mPa·s) of Ionic Liquid $[C_6mim][NTf_2]$ Using the Force Field Developed in This Work Together with Experimental Values at Different Temperatures

T/K	simulations	experiments ⁹¹
298	119	69.9
313	71	37.0
323	41	25.9
333	25	19.0
343	21	14.4
353	15.5	11.2
363	10.3	8.97
373	8.0	7.33

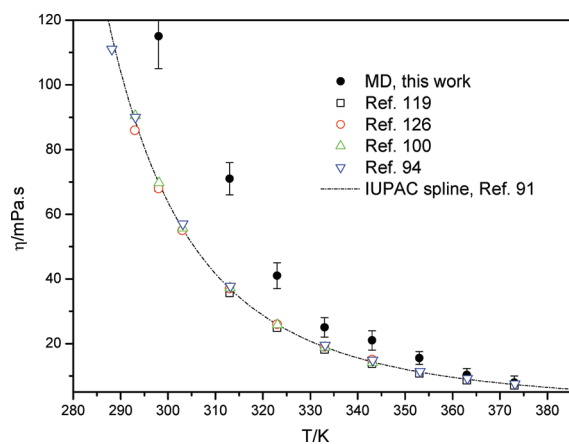


Figure 10. Temperature dependence of the viscosity for ionic liquid $[C_6mim][Tf_2N]$. Simulated values using the force field developed in this work (solid circles) are compared with experimental measurements (open symbols). The dashed line is drawn by the recommended correlated equations in ref 91.

used to calculate the viscosity. The block-averaging method was used to obtain the viscosity and estimate the corresponding error bars. Figure S5 in the Supporting Information shows a typical determination of viscosity by the plateau of the integral of the correlation function. The details of the calculation can be found in our previous work.^{71,89}

Table 7 shows the predicted viscosities of ILs studied in this work as well as the corresponding experimental values.^{103,118,119,125,126} The simulated values agree well with the experiments. As shown in Figure 9, the alkyl length dependence of the viscosities of the $[C_nmim][NTf_2]$ family ILs is well predicted by our force field, in which a minimum of the viscosity at $n = 2$ is found in both the simulations and the experiments. For ILs with other anions, the force field gives slightly higher values in most cases, typically with deviations less than 50%. The largest deviation of about two times overestimation was found in the results of $[C_4mim][CH_3SO_4]$.

The simulated viscosities of $[C_6mim][NTf_2]$ as a function of temperature are summarized in Table 8. As shown in Figure 10, the simulated values are in good agreement with the experiments⁹¹ at higher temperatures. The deviations between the simulations and experiments increase with the decrease of temperature, which is consistent with the results of the self-diffusion coefficients.

6. CONCLUSIONS

We proposed a cost-effective, classical united-atom (UA) force field for ionic liquids (ILs) composed by 1-alkyl-3-methyl-imidazolium cations ($[C_nmim]^+$, $n = 1\text{--}10$) and seven kinds of anions, including tetrafluoroborate ($[BF_4]^-$), hexafluorophosphate ($[PF_6]^-$), methylsulfate ($[CH_3SO_4]^-$), trifluoromethylsulfonate ($[CF_3SO_3]^-$), acetate ($[CH_3CO_2]^-$), trifluoroacetate ($[CF_3CO_2]^-$), and bis(trifluoromethylsulfonyl)amide ($[NTf_2]^-$). The optimization of parameters of the force fields is based on the strategy in our previous work, in which the effective atom partial charges were used to account for the overall effects of polarization in ILs. These charges were determined by fitting the electrostatic potential surface (ESP) of ion pair dimers, resulting in total charges (absolute values) on cations or anions being less than 1. The partial charges derived from RESP fitting to ion pair dimers and rescaled to $\pm 0.8e$ for all kind of ions by a compromise between transferability and accuracy.

Molecular dynamics (MD) simulations were performed over a wide range of temperatures to validate the force field. The liquid densities were predicted very well for all of the ILs studied in this work in the temperature range of 298–373 K, with typical deviations less than 1%. For the $[C_nmim][NTf_2]$ family ILs, the simulated enthalpies of vaporization, ΔH^{vap} , are also in good agreement with the measured values by different experimental methods reported recently, with slight overestimation about 5 kJ/mol. Our force field predicted that the enthalpy of vaporization increases by about 3.7 kJ/mol per CH_2 group for the $[C_nmim][NTf_2]$ family, which coincides very well with the experimental values of 3.5–3.8 kJ/mol.

More critical validations were made by comparing the transport properties, including the self-diffusion coefficient and shear viscosity, between simulation and experiments. The simulations are carried out long enough (20–60 ns) to estimate the transport properties by equilibrium MD method. The simulated self-diffusion coefficients and viscosities for all the ILs studied in this work are in good agreement with experiments, although slightly lower dynamics is predicted by the force field. The alkyl length and temperature dependence of the properties is also well reproduced in simulations. The deviation between simulation and experiment increases with the increase of the alkyl length and decrease of the temperature. The largest underestimation of the self-diffusion coefficient is about one-third of the experimental values, while the largest overestimation of the viscosity is about two times the experimental values, as found in the results of $[C_6mim][NTf_2]$ at 298 K.

Rai and Maginn¹²⁷ studied the vapor–liquid coexistence curves and critical points of $[C_nmim][BF_4]$ by the force field proposed in this work. The simulated critical point are in very good agreement with those extrapolated from low-temperature experimental surface tension and density data by using both the Eötvös and the Guggenheim models.¹²⁸ The results are encouraging because the phase equilibrium is critically important in chemical process design in which ionic liquid is potentially applied as a promising solvent. We also carried out extensive MD simulations of $[C_4mim][BF_4] + H_2O$ mixtures. Preliminary results show good performance on the excess properties, which are very sensitive to the force field. A detailed analysis of the mixtures properties is also in progress.

■ ASSOCIATED CONTENT

S Supporting Information. All parameters of the force field; comparisons of bond and angle distributions between the

united-atom and all-atom models, by which we fit the equilibrium length of the UA bond and angles; comparisons of the radial distribution function of CF₃-CF₃ calculated from AA and UA models; values of β and self-diffusion coefficients of [C₆mim]-[NTf₂] by fitting different time spans of MSD at 298 and 373 K; typical integral of the correlation function (see eq 6) used to estimate the viscosity; optimized structures of ion pair dimers (see section 2.3). This material is available free of charge via the Internet at <http://pubs.acs.org>.

AUTHOR INFORMATION

Corresponding Author

*E-mail: liuzhp@mail.buct.edu.cn (Z.L.), caodp@mail.buct.edu.cn (D.C.).

ACKNOWLEDGMENT

Financial support of the Natural Science Foundation in China (Nos. 20676005, 20976004, and 20736005) is gratefully acknowledged. We also are thankful for the computational resources provided by the Supercomputing Center of China Academic of Sciences (CAS) and Chemical Engineering Grid Computing Center in the Beijing University of Chemical Technology.

REFERENCES

- (1) Welton, T. *Chem. Rev.* **1999**, *99*, 2071–2083.
- (2) Weingaertner, H. *Angew. Chem., Int. Ed.* **2008**, *47*, 654–670.
- (3) Plechkova, N. V.; Seddon, K. R. *Chem. Soc. Rev.* **2008**, *37*, 123–150.
- (4) Bates, E. D.; Mayton, R. D.; Ntai, I.; Davis, J. H. *J. Am. Chem. Soc.* **2002**, *124*, 926–927.
- (5) Zhu, A. L.; Jiang, T.; Han, B. X.; Huang, J.; Zhang, J. C.; Ma, X. M. *New J. Chem.* **2006**, *30*, 736–740.
- (6) Yu, G. R.; Zhang, S. J.; Yao, X. Q.; Zhang, J. M.; Dong, K.; Dai, W. B.; Mori, R. *Ind. Eng. Chem. Res.* **2006**, *45*, 2875–2880.
- (7) Lee, S. G. *Chem. Commun.* **2006**, 1049–1063.
- (8) Wang, C. M.; Luo, H. M.; Jiang, D. E.; Li, H. R.; Dai, S. *Angew. Chem., Int. Ed.* **2010**, *49*, 5978–5981.
- (9) Giernoth, R. *Angew. Chem., Int. Ed.* **2010**, *49*, 2834–2839.
- (10) Parvulescu, V. I.; Hardacre, C. *Chem. Rev.* **2007**, *107*, 2615–2665.
- (11) Hagfeldt, A.; Boschloo, G.; Sun, L. C.; Kloo, L.; Pettersson, H. *Chem. Rev.* **2010**, *110*, 6595–6663.
- (12) Kuang, D.; Brillet, J.; Chen, P.; Takata, M.; Uchida, S.; Miura, H.; Sumioka, K.; Zakeeruddin, S. M.; Gratzel, M. *ACS Nano* **2008**, *2*, 1113–1116.
- (13) Zhang, S. J.; Chen, Y. H.; Li, F. W.; Lu, X. M.; Dai, W. B.; Mori, R. *Catal. Today* **2006**, *115*, 61–69.
- (14) Bara, J. E.; Camper, D. E.; Gin, D. L.; Noble, R. D. *Acc. Chem. Res.* **2010**, *43*, 152–159.
- (15) Karadas, F.; Atilhan, M.; Aparicio, S. *Energy Fuels* **2010**, *24*, 5817–5828.
- (16) Swatloski, R. P.; Spear, S. K.; Holbrey, J. D.; Rogers, R. D. *J. Am. Chem. Soc.* **2002**, *124*, 4974–4975.
- (17) Zhang, H.; Wu, J.; Zhang, J.; He, J. S. *Macromolecules* **2005**, *38*, 8272–8277.
- (18) Rinaldi, R.; Palkovits, R.; Schuth, F. *Angew. Chem., Int. Ed.* **2008**, *47*, 8047–8050.
- (19) Yong, G.; Zhang, Y. G.; Ying, J. Y. *Angew. Chem., Int. Ed.* **2008**, *47*, 9345–9348.
- (20) Yang, W.; Fellinger, T. P.; Antonietti, M. *J. Am. Chem. Soc.* **2011**, *133*, 206–209.
- (21) Ma, Z.; Yu, J. H.; Dai, S. *Adv. Mater.* **2010**, *22*, 261–285.
- (22) Maginn, E. J. *AIChE J.* **2009**, *55*, 1304–1310.
- (23) Klamt, A.; Eckert, F.; Arlt, W. COSMO-RS: An Alternative to Simulation for Calculating Thermodynamic Properties of Liquid Mixtures. In *Annual Review of Chemical and Biomolecular Engineering*, Vol 1, Annual Reviews: Palo Alto, 2010; Vol. 1, pp 101–122.
- (24) Zhang, X. C.; Liu, Z. P.; Wang, W. C. *AIChE J.* **2008**, *54*, 2717–2728.
- (25) Lynden-Bell, R. M.; Del Popolo, M. G.; Youngs, T. G. A.; Kohanoff, J.; Hanke, C. G.; Harper, J. B.; Pinilla, C. C. *Acc. Chem. Res.* **2007**, *40*, 1138–1145.
- (26) Maginn, E. J. *J. Phys.: Condens. Matter* **2009**, *21*, 373101.
- (27) Hunt, P. A. *Mol. Simul.* **2006**, *32*, 1–10.
- (28) Bhargava, B. L.; Balasubramanian, S.; Klein, M. L. *Chem. Commun.* **2008**, 3339–3351.
- (29) Hanke, C. G.; Price, S. L.; Lynden-Bell, R. M. *Mol. Phys.* **2001**, *99*, 801–809.
- (30) Lopes, J. N. C.; Deschamps, J.; Padua, A. A. H. *J. Phys. Chem. B* **2004**, *108*, 2038–2047.
- (31) Lopes, J. N. C.; Padua, A. A. H. *J. Phys. Chem. B* **2004**, *108*, 16893–16898.
- (32) Lopes, J. N. C.; Padua, A. A. H. *J. Phys. Chem. B* **2006**, *110*, 19586–19592.
- (33) Lopes, J. N. C.; Padua, A. A. H.; Shimizu, K. *J. Phys. Chem. B* **2008**, *112*, 5039–5046.
- (34) Shimizu, K.; Almantariotis, D.; Gomes, M. F. C.; Padua, A. A. H.; Lopes, J. N. C. *J. Phys. Chem. B* **2010**, *114*, 3592–3600.
- (35) Morrow, T. I.; Maginn, E. J. *J. Phys. Chem. B* **2002**, *106*, 12807–12813.
- (36) Cadena, C.; Zhao, Q.; Snurr, R. Q.; Maginn, E. J. *J. Phys. Chem. B* **2006**, *110*, 2821–2832.
- (37) Cadena, C.; Maginn, E. J. *J. Phys. Chem. B* **2006**, *110*, 18026–18039.
- (38) Liu, Z. P.; Huang, S. P.; Wang, W. C. *J. Phys. Chem. B* **2004**, *108*, 12978–12989.
- (39) Liu, Z. P.; Wu, X. P.; Wang, W. C. *Phys. Chem. Chem. Phys.* **2006**, *8*, 1096–1104.
- (40) Liu, X. M.; Zhang, S. J.; Zhou, G. H.; Wu, G. W.; Yuan, X. L.; Yao, X. Q. *J. Phys. Chem. B* **2006**, *110*, 12062–12071.
- (41) Zhou, G. H.; Liu, X. M.; Zhang, S. J.; Yu, G. G.; He, H. Y. *J. Phys. Chem. B* **2007**, *111*, 7078–7084.
- (42) Tsuzuki, S.; Umecky, T.; Matsumoto, H.; Shinoda, W.; Mikami, M. *J. Phys. Chem. B* **2010**, *114*, 11390–11396.
- (43) Sambasivaran, S. V.; Acevedo, O. J. *Chem. Theory Comput.* **2009**, *5*, 1038–1050.
- (44) Micaelo, N. M.; Baptista, A. M.; Soares, C. M. *J. Phys. Chem. B* **2006**, *110*, 14444–14451.
- (45) Hu, Z. H.; Margulis, C. J. *Acc. Chem. Res.* **2007**, *40*, 1097–1105.
- (46) Lopes, J.; Padua, A. A. H. *J. Phys. Chem. B* **2006**, *110*, 3330–3335.
- (47) Chaumont, A.; Wipff, C. *J. Phys. Chem. B* **2010**, *114*, 13773–13785.
- (48) Izgorodina, E. I. *Phys. Chem. Chem. Phys.* **2011**, *13*, 4189–4207.
- (49) Dommert, F.; Schmidt, J.; Qiao, B. F.; Zhao, Y. Y.; Krekeler, C.; Delle Site, L.; Berger, R.; Holm, C. *J. Chem. Phys.* **2008**, *129*, 224501.
- (50) Tsuzuki, S.; Shinoda, W.; Saito, H.; Mikami, M.; Tokuda, H.; Watanabe, M. *J. Phys. Chem. B* **2009**, *113*, 10641–10649.
- (51) Yan, T. Y.; Burnham, C. J.; Del Popolo, M. G.; Voth, G. A. *J. Phys. Chem. B* **2004**, *108*, 11877–11881.
- (52) Yan, T. Y.; Wang, Y. T.; Knox, C. *J. Phys. Chem. B* **2010**, *114*, 6886–6904.
- (53) Yan, T. Y.; Wang, Y. T.; Knox, C. *J. Phys. Chem. B* **2010**, *114*, 6905–6921.
- (54) Borodin, O.; Smith, G. D. *J. Phys. Chem. B* **2006**, *110*, 11481–11490.
- (55) Borodin, O. *J. Phys. Chem. B* **2009**, *113*, 11463–11478.
- (56) Bedrov, D.; Borodin, O.; Li, Z.; Smith, G. D. *J. Phys. Chem. B* **2010**, *114*, 4984–4997.
- (57) Schroder, C.; Steinhauser, O. *J. Chem. Phys.* **2010**, *133*, 154511.
- (58) Chang, T. M.; Dang, L. X. *J. Phys. Chem. A* **2009**, *113*, 2127–2135.
- (59) Tanaka, M.; Siehl, H. U. *Chem. Phys. Lett.* **2008**, *457*, 263–266.

- (60) Nakano, H.; Yamamoto, T.; Kato, S. *J. Chem. Phys.* **2010**, *132*, 044106.
- (61) Youngs, T. G. A.; Hardacre, C. *ChemPhysChem* **2008**, *9*, 1548–1558.
- (62) Lee, S. U.; Jung, J.; Han, Y. K. *Chem. Phys. Lett.* **2005**, *406*, 332–340.
- (63) Logothetis, G. E.; Ramos, J.; Economou, I. G. *J. Phys. Chem. B* **2009**, *113*, 7211–7224.
- (64) Bhargava, B. L.; Balasubramanian, S. *J. Chem. Phys.* **2007**, *127*.
- (65) Wei, Z.; Leroy, F.; Balasubramanian, S.; Muller-Plathe, F. *J. Phys. Chem. B* **2008**, *112*, 8129–8133.
- (66) Klahn, M.; Seduraman, A.; Wu, P. *J. Phys. Chem. B* **2008**, *112*, 10989–11004.
- (67) Klahn, M.; Seduraman, A.; Wu, P. *J. Phys. Chem. B* **2008**, *112*, 13849–13861.
- (68) Roy, D.; Maroncelli, M. *J. Phys. Chem. B* **2010**, *114*, 12629–12631.
- (69) Koddermann, T.; Paschek, D.; Ludwig, R. *ChemPhysChem* **2007**, *8*, 2464–2470.
- (70) Emel'yanenko, V. N.; Verevkin, S. P.; Heintz, A.; Schick, C. *J. Phys. Chem. B* **2008**, *112*, 8095–8098.
- (71) Liu, Z. P.; Chen, T.; Bell, A.; Smit, B. *J. Phys. Chem. B* **2010**, *114*, 4572–4582.
- (72) Bayly, C. I.; Cieplak, P.; Cornell, W. D.; Kollman, P. A. *J. Phys. Chem.* **1993**, *97*, 10269–10280.
- (73) Schmidt, J.; Krekeler, C.; Dommert, F.; Zhao, Y. Y.; Berger, R.; Delle Site, L.; Holm, C. *J. Phys. Chem. B* **2010**, *114*, 6150–6155.
- (74) Krekeler, C.; Dommert, F.; Schmidt, J.; Zhao, Y. Y.; Holm, C.; Berger, R.; Delle Site, L. *Phys. Chem. Chem. Phys.* **2010**, *12*, 1817–1821.
- (75) Mele, A.; Tran, C. D.; Lacerda, S. H. D. *Angew. Chem., Int. Ed.* **2003**, *42*, 4364–4366.
- (76) Dong, K.; Zhang, S. J.; Wang, D. X.; Yao, X. Q. *J. Phys. Chem. A* **2006**, *110*, 9775–9782.
- (77) Wang, J. M.; Wolf, R. M.; Caldwell, J. W.; Kollman, P. A.; Case, D. A. *J. Comput. Chem.* **2004**, *25*, 1157–1174.
- (78) Wu, X. P.; Liu, Z. P.; Huang, S. P.; Wang, W. C. *Phys. Chem. Chem. Phys.* **2005**, *7*, 2771–2779.
- (79) Angenendt, K.; Johansson, P. *J. Phys. Chem. C* **2010**, *114*, 20577–20582.
- (80) Frisch, M. J.; Trucks, G. W.; Schlegel, H. B.; Scuseria, G. E.; Robb, M. A.; Cheeseman, J. R.; Montgomery, Jr., J. A.; Vreven, T.; Kudin, K. N.; Burant, J. C.; Millam, J. M.; Iyengar, S. S.; Tomasi, J.; Barone, V.; Mennucci, B.; Cossi, M.; Scalmani, G.; Rega, N.; Petersson, G. A.; Nakatsuji, H.; Hada, M.; Ehara, M.; Toyota, K.; Fukuda, R.; Hasegawa, J.; Ishida, M.; Nakajima, T.; Honda, Y.; Kitao, O.; Nakai, H.; Klene, M.; Li, X.; Knox, J. E.; Hratchian, H. P.; Cross, J. B.; Bakken, V.; Adamo, C.; Jaramillo, J.; Gomperts, R.; Stratmann, R. E.; Yazayev, O.; Austin, A. J.; Cammi, R.; Pomelli, C.; Ochterski, J. W.; Ayala, P. Y.; Morokuma, K.; Voth, G. A.; Salvador, P.; Dannenberg, J. J.; Zakrzewski, V. G.; Dapprich, S.; Daniels, A. D.; Strain, M. C.; Farkas, O.; Malick, D. K.; Rabuck, A. D.; Raghavachari, K.; Foresman, J. B.; Ortiz, J. V.; Cui, Q.; Baboul, A. G.; Clifford, S.; Cioslowski, J.; Stefanov, B. B.; Liu, G.; Liashenko, A.; Piskorz, P.; Komaromi, I.; Martin, R. L.; Fox, D. J.; Keith, T.; Al-Laham, M. A.; Peng, C. Y.; Nanayakkara, A.; Challacombe, M.; Gill, P. M. W.; Johnson, B.; Chen, W.; Wong, M. W.; Gonzalez, C.; Pople, J. A. *Gaussian 03, Revision C.02*; Gaussian, Inc.: Wallingford, CT, 2004.
- (81) Stoppa, A.; Zech, O.; Kunz, W.; Buchner, R. *J. Phys. Eng. Data* **2010**, *55*, 1768–1773.
- (82) Taguchi, R.; Machida, H.; Sato, Y.; Smith, R. L. *J. Chem. Eng. Data* **2009**, *54*, 22–27.
- (83) Walser, R.; Mark, A. E.; van Gunsteren, W. F.; Lauterbach, M.; Wipff, G. *J. Chem. Phys.* **2000**, *112*, 10450–10459.
- (84) Shelley, J. C.; Shelley, M. Y.; Reeder, R. C.; Bandyopadhyay, S.; Klein, M. L. *J. Phys. Chem. B* **2001**, *105*, 4464–4470.
- (85) Martin, M. G.; Siepmann, J. I. *J. Phys. Chem. B* **1998**, *102*, 2569–2577.
- (86) Cui, S. T.; Siepmann, J. I.; Cochran, H. D.; Cummings, P. T. *Fluid Phase Equilib.* **1998**, *146*, 51–61.
- (87) Plimpton, S. J. *J. Comput. Phys.* **1995**, *117*, 1–19 <http://lammps.sandia.gov/>.
- (88) Martínez, L.; Andrade, R.; Birgin, E. G.; Martínez, J. M. *J. Comput. Chem.* **2009**, *30*, 2157–2164.
- (89) Chen, T.; Smit, B.; Bell, A. T. *J. Chem. Phys.* **2009**, *131*, 246101.
- (90) Marsh, K. N.; Brennecke, J. F.; Chirico, R. D.; Frenkel, M.; Heintz, A.; Magee, J. W.; Peters, C. J.; Rebelo, L. P. N.; Seddon, K. R. *Pure Appl. Chem.* **2009**, *81*, 781–790.
- (91) Chirico, R. D.; Diky, V.; Magee, J. W.; Frenkel, M.; Marsh, K. N. *Pure Appl. Chem.* **2009**, *81*, 791–828.
- (92) Krummen, M.; Wasserscheid, P.; Gmehling, J. *J. Chem. Eng. Data* **2002**, *47*, 1411–1417.
- (93) Gardas, R. L.; Freire, M. G.; Carvalho, P. J.; Marrucho, I. M.; Fonseca, I. M. A.; Ferreira, A. G. M.; Coutinho, J. A. P. *J. Chem. Eng. Data* **2007**, *52*, 1881–1888.
- (94) Kandil, M. E.; Marsh, K. N.; Goodwin, A. R. H. *J. Chem. Eng. Data* **2007**, *52*, 2382–2387.
- (95) Jacquemin, J.; Husson, P.; Mayer, V.; Cibulka, I. *J. Chem. Eng. Data* **2007**, *52*, 2204–2211.
- (96) Kato, R.; Gmehling, J. *J. Chem. Thermodyn.* **2005**, *37*, 603–619.
- (97) Tome, L. I. N.; Carvalho, P. J.; Freire, M. G.; Marrucho, I. M.; Fonseca, I. M. A.; Ferreira, A. G. M.; Coutinho, J. A. P.; Gardas, R. L. *J. Chem. Eng. Data* **2008**, *53*, 1914–1921.
- (98) Soriano, A. N.; Doma, B. T.; Li, M. H. *J. Chem. Thermodyn.* **2009**, *41*, 301–307.
- (99) Gardas, R. L.; Freire, M. G.; Carvalho, P. J.; Marrucho, I. M.; Fonseca, I. M. A.; Ferreira, A. G. M.; Coutinho, J. A. P. *J. Chem. Eng. Data* **2007**, *52*, 80–88.
- (100) Tokuda, H.; Tsuzuki, S.; Susan, M.; Hayamizu, K.; Watanabe, M. *J. Phys. Chem. B* **2006**, *110*, 19593–19600.
- (101) Li, W. J.; Zhang, Z. F.; Han, B. X.; Hu, S. Q.; Xie, Y.; Yang, G. Y. *J. Phys. Chem. B* **2007**, *111*, 6452–6456.
- (102) Shiflett, M. B.; Kasprzak, D. J.; Junk, C. P.; Yokozeki, A. *J. Chem. Thermodyn.* **2008**, *40*, 25–31.
- (103) Pereiro, A. B.; Verdia, P.; Tojo, E.; Rodriguez, A. *J. Chem. Eng. Data* **2007**, *52*, 377–380.
- (104) Jorgensen, W. L.; Maxwell, D. S.; TiradoRives, J. *J. Am. Chem. Soc.* **1996**, *118*, 11225–11236.
- (105) Esperanca, J.; Lopes, J. N. C.; Tariq, M.; Santos, L.; Magee, J. W.; Rebelo, L. P. N. *J. Chem. Eng. Data* **2010**, *55*, 3–12.
- (106) Zaitsau, D. H.; Kabo, G. J.; Strechan, A. A.; Paulechka, Y. U.; Tschersich, A.; Verevkin, S. P.; Heintz, A. *J. Phys. Chem. A* **2006**, *110*, 7303–7306.
- (107) Santos, L.; Lopes, J. N. C.; Coutinho, J. A. P.; Esperanca, J.; Gomes, L. R.; Marrucho, I. M.; Rebelo, L. P. N. *J. Am. Chem. Soc.* **2007**, *129*, 284–285.
- (108) Armstrong, J. P.; Hurst, C.; Jones, R. G.; Licence, P.; Lovelock, K. R. J.; Satterley, C. J.; Villar-Garcia, I. *J. Phys. Chem. Chem. Phys.* **2007**, *9*, 982–990.
- (109) Emel'yanenko, V. N.; Verevkin, S. P.; Heintz, A. *J. Am. Chem. Soc.* **2007**, *129*, 3930–3937.
- (110) Luo, H. M.; Baker, G. A.; Dai, S. *J. Phys. Chem. B* **2008**, *112*, 10077–10081.
- (111) Koddermann, T.; Paschek, D.; Ludwig, R. *Chemphyschem* **2008**, *9*, 549–555.
- (112) Kelkar, M. S.; Maginn, E. J. *J. Phys. Chem. B* **2007**, *111*, 9424–9427.
- (113) Borodin, O. *J. Phys. Chem. B* **2009**, *113*, 12353–12357.
- (114) Shimizu, K.; Tariq, M.; Gomes, M. F. C.; Rebelo, L. P. N.; Lopes, J. N. C. *J. Phys. Chem. B* **2010**, *114*, 5831–5834.
- (115) Paulechka, Y. U. *J. Phys. Chem. Ref. Data* **2010**, *39*.
- (116) Paulechka, Y. U.; Kabo, G. J.; Emel'yanenko, V. N. *J. Phys. Chem. B* **2008**, *112*, 15708–15717.
- (117) Schroder, C.; Steinhauser, O. *J. Chem. Phys.* **2008**, *128*, 224503.
- (118) Tokuda, H.; Hayamizu, K.; Ishii, K.; Abu Bin Hasan Susan, M.; Watanabe, M. *J. Phys. Chem. B* **2004**, *108*, 16593–16600.
- (119) Tokuda, H.; Hayamizu, K.; Ishii, K.; Susan, M.; Watanabe, M. *J. Phys. Chem. B* **2005**, *109*, 6103–6110.

- (120) Daivis, P. J.; Evans, D. J. *J. Chem. Phys.* **1994**, *100*, 541–547.
- (121) Mondello, M.; Grest, G. S. *J. Chem. Phys.* **1997**, *106*, 9327–9336.
- (122) Borodin, O.; Smith, G. D.; Kim, H. *J. Phys. Chem. B* **2009**, *113*, 4771–4774.
- (123) Chen, T.; Chidambaram, M.; Lin, Z. P.; Smit, B.; Bell, A. T. *J. Phys. Chem. B* **2010**, *114*, 5790–5794.
- (124) Van-Oanh, N. T.; Houriez, C.; Rousseau, B. *Phys. Chem. Chem. Phys.* **2010**, *12*, 930–936.
- (125) Almantariotis, D.; Gefflaut, T.; Padua, A. A. H.; Coxam, J. Y.; Gomes, M. F. C. *J. Phys. Chem. B* **2010**, *114*, 3608–3617.
- (126) Crosthwaite, J. M.; Muldoon, M. J.; Dixon, J. K.; Anderson, J. L.; Brennecke, J. F. *J. Chem. Thermodyn.* **2005**, *37*, 559–568.
- (127) Rai, N.; Maginn, E. J. *J. Phys. Chem. Lett.* **2011**, *2*, 1439–1443.
- (128) Rebelo, L. P. N.; Lopes, J. N. C.; Esperanca, J.; Filipe, E. *J. Phys. Chem. B* **2005**, *109* (13), 6040–6043.